Natural variation in stomata size contributes to the local adaptation of water-use efficiency in *Arabidopsis thaliana*

H. Dittberner[1], A. Korte[2], T. Mettler-Altmann[3], A.P.M. Weber[3], G. Monroe[4], J. de Meaux[1]

Affiliations: [1]Institute of Botany, University of Cologne, 50674 Cologne; [2]Center for Computational and Theoretical Biology, Julius-Maximilians-University Würzburg, 97074 Würzburg; [3]Institute of Plant Biochemistry & CEPLAS Plant Metabolism and Metabolomics Laboratory, Heinrich-Heine-University Düsseldorf, 40225 Düsseldorf; [4]College of Agricultural Sciences, Colorado State University, Fort Collins, CO 80523-1101

Abstract

Stomata control gas exchanges between the plant and the atmosphere. How natural variation in stomata size and density contributes to resolve trade-offs between carbon uptake and water-loss in response to local climatic variation is not yet understood. We developed an automated confocal microscopy approach to characterize natural genetic variation in stomatal patterning in 330 fully-sequenced *Arabidopsis thaliana* ecotypes collected throughout the European range of the species. We compared this to variation in water-use efficiency, measured as carbon isotope discrimination ($\delta^{13}C$). Combined with public genomic and environmental resources, we show that genetic variation for stomata size and density is pervasive in *Arabidopsis thaliana*. A positive correlation between stomata size and $\delta^{13}C$ further shows that this variation has consequences on water-use efficiency. Genome-wide association analyses reveal that many loci of small effect contribute not only to variation in stomata patterning but also to its co-variation with carbon uptake parameters. Yet, we report two novel QTL affecting $\delta^{13}C$ independently of stomata patterning. This suggests that, in *A. thaliana*, both morphological and physiological variants contribute to genetic variance in water-use efficiency. Patterns of regional differentiation and co-variation with climatic parameters indicate that natural selection has contributed to shape some of this variation, especially in Southern Sweden, where water availability is comparatively more limited in Spring.

Keywords

GWAS; stomata; water-use efficiency; Arabidopsis thaliana; Q_{ST} F_{ST} analysis; local adaptation to climate

Introduction

Stomata form microscopic pores controlling gas exchange on the surface of plant leaves. These pores provide plants with a strategic lever arm to optimize the trade-off between growth and survival. As the gas exchange organ for higher plants, stomata intimately link three key functional traits: carbon (CO2) uptake, water loss and leaf cooling (Raven, 2002). Therefore, the density, distribution and regulation of stomata, may have played a pivotal role in shaping the diversity of plant communities throughout the globe (Lambers, Chapin, & Pons, 1998; McDowell et al., 2008).

Short term plastic changes in rate of gas exchange (termed stomatal conductance) provide a first level at which the plant manages the conflicting demands on carbon uptake and water loss in the face of daily fluctuations in water and light availability. For this, the two guard cells that form the stomata modulate conductance by modifying their turgor in response to environmental and internal signals (Chater et al., 2011; Kinoshita et al., 2011). This ensures, for example, that plants do not desiccate at high noon when water evaporation is maximal or at night when photosynthesis is not active (Daszkowska-Golec & Szarejko, 2013).

Less well understood, however, is how variation in the arrangement and size of stomata on the leaf surface (stomatal patterns) participates in the resolution of the conflict between water loss and growth. Physical conductance theory predicts that small stomata in high density are required to maximize conductance (Franks & Beerling, 2009). Experimental data, however, do not always support this prediction. A significant relationship between stomatal patterns and conductance has sometimes been reported (Anderson & Briske, 1990; Carlson, Adams, & Holsinger, 2016; Franks & Beerling, 2009; Muchow & Sinclair, 1989; Pearce, Millard, Bray,

& Rood, 2006; Reich, 1984), but is not always detected (Bakker, 1991; Ohsumi, Kanemura, Homma, Horie, & Shiraiwa, 2007).

Much is known about the complex molecular pathway, that controls the differentiation of protodermal cells into stomata, at the expense of classical epidermal cells in the model plant species *Arabidopsis thaliana* (Bergmann & Sack, 2007; Pillitteri & Torii, 2012). Mutants in this pathway show not only modified stomata patterns, but also altered water-use efficiency (WUE), which quantifies a plant's ability to fix carbon while minimizing water loss, or survival after exposure to drought stress (Franks, W. Doheny-Adams, Britton-Harper, & Gray, 2015; Yoo et al., 2010). Thus, genetic modification of stomatal patterning can provide potentially adaptive phenotypes in more arid environments. In addition, stomatal density and size are generally strongly negatively correlated, which may either accelerate or constrain the evolution of the optimal adaptive patterns (reviewed in (Hetherington & Woodward, 2003).

Natural variation of stomatal patterns has been evaluated in various species, showing that it often associates with increased water-use efficiency and environmental variation. In *Protea repens*, when measured in a common garden experiment with 19 populations, stomata density increased with annual mean temperature and decreased with summer rainfall at the source location (Carlson et al., 2016). In species of the *Mimulus guttatus* species complex grown in a common garden, accessions from drier inland populations showed decreased stomatal density associated with an increase in WUE, compared to accessions collected in humid coastal populations (Wu, Lowry, Nutter, & Willis, 2010). In *Eucalyptus globulus*, it is stomata size and not stomata density that associated with water-use efficiency. When *E. globulus* populations were grown in two field sites with contrasting rainfall, plants from the drier site had smaller stomata independent of their density and higher WUE (Franks, Drake, &

Beerling, 2009). This suggested that developmental correlation between stomata size and density may sometimes be alleviated to better match physiological performance with local environments.

Stomatal patterning also affects the efficiency of the short-term response of stomatal aperture to stress. In the *Banksia* genus, species with smaller stomata and higher densities were able to open stomata faster in response to light (Drake, Froend, & Franks, 2013). Stomatal responses are an order of magnitude slower than photosynthetic changes, and the increased time lag of larger stomata may favor water loss and reduce WUE (T. Lawson, Kramer, & Raines, 2012). The plastic decrease in stomata length observed in diverse populations of *Arabidopsis lyrata ssp. lyrata* in response to water limitations indeed correlated with an increase in WUE (Paccard, Fruleux, & Willi, 2014). Thus, increased stomata density can, counterintuitively, contribute to improved WUE since it decreases stomata size, and in turn favors faster opening/closing reactions. Therefore, the natural variation reported for stomatal traits in various plant species, appears to have complex consequences on both physiological performance and the associations with diverse environmental factors. Yet, without an understanding of the underlying genetic architecture, the question of the adaptive relevance of stomatal patterning and its ecological drivers remains unresolved.

Eco-evolutionary analyses provide a powerful approach to establish the ecological importance of specific traits (Carroll, Hendry, Reznick, & Fox, 2007; Hendry, 2016). By drawing on the elaborate toolbox of population genetics and genomics, it is not only possible to test whether a given trait is genetically variable, but also to ask whether it is optimized by natural selection and to investigate the ecological determinants of the selective forces at work (Hendry, 2016; Weinig, Ewers, & Welch, 2014). In this effort, the annual species *Arabidopsis thaliana*, which thrives as a pioneer species in disturbed habitats, has a privileged position (Gaut,

2012). Ecotypes of *A. thaliana* show a high degree of variation in many vital phenotypic traits, which is at least partly shaped by local adaptation (Ågren & Schemske, 2012; Baxter et al., 2010; Fournier-Level et al., 2011; Postma & Ågren, 2016; Stinchcombe et al., 2004). This diversity and the availability of over 1000 fully sequenced accessions (Alonso-Blanco et al., 2016) make it an ideal species for studying ecological adaptation of plants. Indeed, genome-wide patterns of nucleotide variation can be contrasted to phenotypic variation and both the genetic architecture and the adaptive history of the traits can be reconstructed (Atwell et al., 2010; Fournier-Level et al., 2011). Eco-evolutionary approaches have allowed documenting for example the adaptive importance of seed dormancy for summer drought avoidance (Kronholm, Picó, Alonso-Blanco, Goudet, & Meaux, 2012), the adaptive re-modeling of trade-offs between life-history traits across the species range (Debieu et al., 2013), the importance of pre-adaptation to climate for biological invasions (Hamilton, Okada, Korves, & Schmitt, 2015) or the ecological importance of plasticity to environmental stress (Lasky et al., 2014).

Natural variation in stomatal patterning is known to segregate in *Arabidopsis thaliana* (Delgado, Alonso-Blanco, Fenoll, & Mena, 2011), but so far technical limitations have complicated the phenotyping of stomatal variation on larger samples. Here, we developed an automated confocal microscopy approach that overcomes this limitation and characterized genetic variation in stomatal patterning in 330 fully-sequenced accessions, across a North-South transect of the European range. Additionally, we measured $\delta^{13}C$, a measure of water-use efficiency, for all genotypes. Combined with public genomic and environmental resources, this dataset allows us to ask i) how much genetic variation of stomata patterns is in natural *A. thaliana* populations? ii) does variation in stomata patterning influence the carbon-water trade-off, iii) what is the genetic architecture of stomata variation? iv) is variation in

stomata patterning impacted by natural selection and v) what ecological parameters determine the selective force?

We find that genetic variation for stomata size correlates negatively with both stomata density and water-use efficiency, reflected by $\delta^{13}C$. Using estimates from multi-trait mixed models (MTMM, (Korte et al., 2012), we show that the correlation between stomata size and $\delta^{13}C$ is determined by a common, yet highly polygenic genetic basis. The correlation between stomata size and density, instead, did not show a detectable common genetic basis. In addition, genome-wide association studies (GWAS) revealed two novel QTL that control $\delta^{13}C$ independent of stomata size. We conclude that stomatal patterning contributes to some of the modulation of water-use efficiency. Patterns of variation with environmental variables suggest, nevertheless, that each of these traits evolves under local selective pressures.

Methods

Plant material, plant genotypes and growth conditions

In total, 330 accessions, spanning a wide geographical range were selected from the 1001 collection of fully sequenced genotypes (Suppl. Table 1). Accessions were assigned to 5 groups based on their geographic origin: Spain, Western Europe, Central Europe, South Sweden and North Sweden (Figure S1). The genome sequences of the 330 genotypes included in the analysis were downloaded from the 1001 genome database (Alonso-Blanco et al., 2016) on May 12th, 2017. For population genomic analysis, single Nucleotide Polymorphism (SNP) data were extracted using *vcftools* (Danecek et al., 2011). SNPs were randomly thinned to one variant per kilobase, which is the approximate extent of linkage disequilibrium in *A. thaliana* (Nordborg et al., 2002). Additionally, minimum minor allele frequency was set to 5% and sites with more than 5% missing data were removed, resulting in 70,410 SNPs among all

genotypes. SNP information was loaded into R using the *vcfR* package (Knaus, Grunwald, Anderson, Winter, & Kamvar, 2017). For genome-wide association studies the full SNP data set was used and missing SNPs were imputed using BEAGLE version 3.0 (Browning & Browning, 2009).

Seeds were stratified on wet paper for 6 days at 4°C in the dark. Plants were grown on soil in 5x5cm paper pots in 3 replicates with one plant per pot. Genotypes were randomized within each of 3 blocks of 12 trays containing 8x4 pots. Plants were grown for 7 weeks in growth chambers (one for each block) under following conditions: 16h light; 95 µmol s□¹ mm□² light intensity; 20 °C day temperature and 18 °C night temperature. Plants were watered twice a week and trays were shuffled and rotated every two to three days to account for variable conditions within the chambers.

High throughput microscopy

After 7 weeks, one fully-expanded intact adult leaf (one of the largest leaves that developed after leaf 4) was selected on each plant for microscopic analysis. From each leaf, two discs were cut mid-way along the length of the leaf on both sides of the main vein, using a 6mm hole punch. If the leaf was too small to cut two discs an additional leaf was collected. The discs were loaded onto an array of 80 spring mounted stamps with the abaxial side up and fixed on a thin layer of dental adhesive cream (blend-a-dent Super-Haftcreme). The leaf discs were stained using 25µl of a 100µg/ml propidium iodide solution for specific staining of stomata and cell walls (Fitzgibbon et al., 2013). A Zellkontakt 96-well glass-bottom plate was then put on top of the stamp array and fixed using four screws. To infiltrate the leaf discs with the stain, the plate was put under vacuum three times for one minute. Microscopic images

were taken using the Opera High Content Screening System from Perkin Elmer. The following settings were used: excitation wavelength 561nm; laser power 11000µW; magnification 20x; camera filter 600/40 nm; dichro filter 568 nm; exposure time 200ms; binning 1. Images were taken in 15 fields (0.15 mm^2) per well/sample. For each field 11 images were taken along the z-axis with 3µm distance to acquire image stacks. In total, we acquired 341,000 microscopic images of abaxial leaf epidermises, resulting in 31,000 image fields for stomata analysis.

Image analysis

The first step of the analysis was performed with the software Acapella from Perkin Elmer. Images were filtered with a sliding parabola filter to reduce background noise. Image stacks were then collapsed to a single 2D image using maximum projection. The stomata detection algorithm was implemented in MATLAB using its Image Processing Toolbox (see Suppl. Document 1 for detailed description). Briefly, images were pre-filtered based on summary statistics to remove low quality images, which could not be analyzed. Images were optimized using noise reduction and contrast enhancement functions and converted to binary images that contained objects (1 pixels) and background (0 pixels), using an intensity threshold. Stomata were among these objects but not exclusively. Hence, they were filtered to remove any false positive detections by using multiple morphological filters based on typical stomata characteristics (e.g. size, shape, etc.).

Stomata phenotypes

For each image, the number of stomata was computed and divided by 0.15 mm² (area of each field) to calculate stomata density. The area (size) of stomata in the image was calculated as the number of pixels of stomata multiplied by the area of a single pixel and a mean stomata size was computed. For each individual plant, the median of each phenotypes over all images was extracted. Stomata density was also determined by counting stomata manually on a random set of 14 individuals as well as on a set of 32 independently-grown individuals. Automatic and manual measurements were strongly correlated (Pearson correlation coefficient $r^2=0.88$, $p<<0.01$and $r^2=0.81$, $p<<0.01$, for the 14 and 32 individuals Figures S 2-3). The algorithm however was conservative and tended to slightly under-estimate stomata numbers. This ensured that stomata area was also correctly quantified.

Leaf size measurements

For leaf size measurements, each hole-punched leaf was fixed on a gridded A4 paper sheet (8 per page) using transparent tape. Possible gaps in the edge of leaves were closed using a pen. Paper sheets were then digitized using a common flatbed scanner. Analysis of the resulting images was performed in MATLAB (see Suppl. Document 1 for detailed description of the algorithm). Images were split into 8 predefined leaf fields and a 4 cm² black reference field was used to determine the true pixel size in mm² for each image. Grayscale values were inverted and the image was converted to binary format using automatic intensity thresholding. Small objects (clutter) were removed using an area opening function. Leaves were identified as large objects of white pixels. Holes in the leaf surface (from the microscopy samples) were

188 closed. Leaf area was measured as the number of white pixels multiplied by the pixel size in
189 mm^2.
190
191
192 ## Carbon isotope discrimination measurements
193 The rosettes of block 1 were placed in individual paper bags after microscopic imaging was
194 completed and dried at 70 °C for 3 weeks. Plant material was then ground to fine powder
195 using a 25mm steel bead and a mixer mill (Retsch, MM 301). Isotope composition was
196 determined using an ISOTOPE cube elemental analyzer coupled to an Isoprime 100 isotope
197 ratio mass spectrometer (both from Elementar, Hanau, Germany) according to (Gowik,
198 Bräutigam, Weber, Weber, & Westhoff, 2011). The carbon isotope ratio is expressed as ‰
199 against the Vienna Pee Dee Belemnite (VPDB) standard.
200
201
202 ## Heritability estimates
203 Broad sense heritability H^2, the proportion of the observed phenotypic variance that is genetic,
204 was estimated as:

$$H^2 = VarG/(VarG + VarE)$$

205 where VarG is the genetic variance and VarE is the environmental variance. Because we
206 worked with inbred lines, the environmental and genetic variance components can be
207 estimated as the variance between replicates of a genotype and the variance between
208 genotypes, respectively, with a linear-mixed-model using block as fixed effect and genotype
209 as random effect. We ran a linear mixed model using the *lme* function from *nlme* package
210 (Pinheiro, Bates, DebRoy, Sarkar, & R Core Team, 2015). For $\delta^{13}C$, no replicates were

211 available but a pseudo-heritability estimate was extracted from the GWAS mixed model
212 including the kinship matrix (Atwell et al., 2010).
213
214

215 ## Genome-Wide Association Study (GWAS)

216 Phenotypic measures including 330 genotypes for stomata density and stomata size, and 310
217 genotypes for $\delta^{13}C$ were deposited in the AraPheno database (Seren et al., 2017). For 261
218 genotypes, all three phenotypes were determined. GWAS was performed for 2.8-3M SNPS
219 with frequency >0.019 with a mixed model correcting for population structure with a kinship
220 matrix calculated under the assumption of the infinitesimal model. Each marker was first
221 analyzed with a fast approximation (Kang et al., 2010) and the 1000 top-most associated
222 SNPs were reanalyzed with the full model following previously described methods (Atwell et
223 al., 2010). R scripts (R Development Core Team, 2008) are available at
224 https://github.com/arthurkorte/GWAS.
225 For trait pairs measured on the same plants, a Multi-trait Mixed Model (MTMM) was applied
226 to distinguish common and trait-specific SNP/phenotype association (Korte et al., 2012) . The
227 MTMM analysis also provides estimates of genetic and environmental correlation for each
228 pair of traits. The R scripts are available at https://github.com/Gregor-Mendel-Institute/mtmm
229 The significance threshold was determined as a Bonferroni threshold, e.g. 0.05 divided by the
230 number of polymorphic SNPs in the dataset.
231
232

Climatic data

Climatic data included average precipitation, temperature, water vapor pressure (humidity), wind speed and solar radiation estimates with 2.5 min grid resolution (WorldClim2 database (Fick & Hijmans, 2017) on May 30th, 2017) and soil water content (Trabucco & Zomer, 2010). For each variable and accession, we extracted a mean over the putative growing season, i.e. the months in the year with average temperature greater than 5 °C and average soil water content over 25% (Suppl. Table 1). We further computed historical drought frequencies at *A. thaliana* collection sites using 30+ years of the remotely-sensed Vegetative Health Index (VHI). The VHI is a drought detection method that combines the satellite measured Vegetative Health and Thermal Condition Indices to identify drought induced vegetative stress globally at weekly, 4km^2 resolution (Kogan, 1995) . This is a validated method for detecting drought conditions in agriculture (Kogan, 1995), which may select for alternative drought tolerance physiologies. Specifically, we used VHI records to calculate the historic frequency of observing drought conditions (VHI<40) during the spring (quarter surrounding spring equinox) and summer (quarter surrounding summer solstice). Spring and summer drought frequencies were transformed into a univariate descriptor of historic drought regimen as the log transformed spring to summer drought frequency ratio. This variable describes the relative risk of experiencing drought in spring vs. summer (Suppl. Table 1). Because these 7 variables are correlated, we combined them in 7 orthogonal principal components for 316 *A. thaliana* collection sites (Figures S4-6, loadings described in Suppl. Document 2). Fourteen genotypes with missing climate data were excluded. Climatic distance between each region pair was estimated as the F-statistic of a multivariate analysis of variance (MANOVA) with climatic PCs as response variables and region of origin as the predictor.

Population genomic analysis

Principal component analysis was done using the *adegenet* package (function *dudi.pca*) (Jombart et al., 2016), with scaled variants (NA converted to mean) (Figures S7-8). Genome-wide F_{ST} estimates were calculated using the *hierfstat* package (function *basic.stats*) (Goudet, 2005). Negative F_{ST} values were set to zero and the 95th percentile was calculated using the *quantile* function.

The phenotypic differentiation between regions, Q_{ST}, was estimated as:

$$Qst = VarB/(VarW + VarB)$$

where VarW is the variance within regions and VarB the variance between regions as decribed in Kronholm et al., 2012. Variance components were estimated with the *lme* function mentioned previously, including block as a fixed effect and genotype within region as a random effect. We used the genotype effect as an estimate for within region variance and the region effect as an estimate for between region variance. Because we did not measure replicates for $\delta^{13}C$, we could not estimate the environmental variance component. Thus, we adapted the model to include only region as a random effect, which was our estimate of between region variance and used the residual variance as within region variance. This approach underestimates Q_{ST} and its use for detecting signatures of local adaptation at the phenotypic level is conservative.

To test whether Q_{ST} estimates significantly exceed the 95th percentile of the F_{ST} distribution, we permuted the phenotypic data in a way that heritability remained constant, e.g. by randomizing genotype labels. For each permutation and phenotype, we calculated the difference between each Q_{ST} value and the 95th percentile of the F_{ST} distribution. We used the

95th percentile of the maximum Q_{ST}-F_{ST} distance distribution as a threshold for determining if phenotypic differentiation significantly exceeds neutral expectations.

Statistical analysis

Statistical analysis was conducted using R (R Development Core Team, 2008) (see Suppl. Document 2 for R Markdown documentation). All plots were created using the *ggplot2* (Wickham, 2009), *ggthemes* (Arnold et al., 2017), *ggmap* (Kahle & Wickham, 2013), *ggbiplot* (Vu, 2011) and *effects* (Fox et al., 2016) libraries.

We used Generalized Linear Models (GLM) to test the effect of block, origin, position in tray and leaf size on each phenotype (stomata density, stomata size and $\delta^{13}C$). Error distribution was a quasipoisson distribution for stomata density and size and a gaussian for $\delta^{13}C$. Stomata density was log-transformed to avoid overdispersion. Significance of each predictor was determined via a type II likelihood-ratio test (*Anova* function of the *car* package). Significant differences between regions were determined with Tukey's contrasts using the *glht* function of the *multcomp* package (Hothorn et al., 2017). GLM Models were also used to test the impact of all climatic principal components on phenotypic traits, while accounting for population structure with the first 20 principal components for genetic variation, which explain 28% of total genetic variation (see above). Additionally, for $\delta^{13}C$ we also tested a simpler model where the climatic parameter was included but not the population structure. From the resulting models, we created effect plots for significant environmental principal components using the *effects* package (Fox et al., 2016).

Results

Significant genetic variation in stomata patterning

We analyzed over 31,000 images collected in three replicate plants of 330 *A. thaliana* genotypes and observed high levels of genetic variation in stomata patterning. Genotypic means ranged from 87 to 204 stomata/mm² for stomata density and from 95.0 µm² to 135.1 µm² for stomata size (see Suppl. Table 2 for raw phenotypic data). Leaf size was not significantly correlated with stomata density (r=-0.02, p=0.7) and stomata size (r=-0.08, p=0.15), as expected in fully developed leaves. Broad-sense heritability (H^2) reached 0.37 and 0.29 for stomata size and density, respectively. Mean stomata density and stomata size were negatively correlated (r=-0.51, p<<0.001; Figure 1), a pattern that has been commonly reported (Hetherington & Woodward, 2003). Due to this strong correlation, we focus primarily on stomata size in the following report, but results for stomata density can be found in the supplemental material.

Stomata size correlates with water-use efficiency

We expected variation in stomatal traits to influence the trade-off between carbon uptake and transpiration. Thus, we measured isotopic carbon discrimination, $\delta^{13}C$, an estimator that increases with water-use efficiency (WUE) (Farquhar, Hubick, Condon, & Richards, 1989; McKay et al., 2008). $\delta^{13}C$ ranged from -38.7‰ to -30.8‰ (Suppl. Table 2) and was significantly correlated with stomata size (r=-0.18, p=0.004; Figure 2), indicating that accessions with smaller stomata have higher WUE. In contrast, we found no significant correlation between stomatal density and $\delta^{13}C$ (r=-0.007, p=0.9, Figure S9).

Common genetic basis of stomata size and $\delta^{13}C$

To identify the genetic basis of the phenotypic variance we observe, we conducted a genome-wide association study (GWAS) for each measured phenotype. Based on the genome-wide nucleotide differences between genotypes (i.e. the kinship matrix), a pseudo-heritability can be calculated. Pseudo-heritability estimates were 0.59 for stomata density, 0.56 for stomata size and 0.69 for $\delta^{13}C$, indicating that differences in stomata patterning and carbon physiology decreased with increasing relatedness. Despite considerable levels of heritability, we did not detect any variant associating with stomata density at a significance above the Bonferroni-corrected p-value of 0.05 (log10(p)=7.78). For stomata size, we detected one QTL with two SNPs significantly associating at positions 8567936 and 8568437 (Figure S10). These SNPs have an allele frequency of 1.5% (5 counts) and 2.1% (7 counts), respectively and map to gene *AT4G14990.1*, which encodes for a protein annotated with a function in cell differentiation. The former SNP is a synonymous coding mutation while the latter is located in an intron. This suggests that variation in stomata size and density is primarily controlled by multiple loci of small effect, with larger effects being contributed by very rare alleles.

For $\delta^{13}C$, one genomic region on chromosome 2 position 15094310 exceeded the Bonferroni significance threshold ($\log_{10}(p)=7.97$, Figure S11). Allele frequency at this SNP was 9.7% (30 counts) and all accessions carrying this allele, except four, were from South Sweden (3 North Sweden, 1 Central Europe). Southern Swedish lines carrying the allele showed significantly increased $\delta^{13}C$ compared to the remaining Southern Swedish lines (W = 1868, p-value = 6.569e-05, Figure S12). A candidate causal mutation is a non-synonymous SNP at position

15109013 in gene *AT2G35970.1*, which codes for a protein belonging to the Late Embryogenesis Abundant (LEA) Hydroxyproline-Rich Glycoprotein family. This SNP also shows elevated association with the phenotype, however its significance lied below the Bonferroni threshold (log(p)=7). Since this SNP is not in linkage disequilibrium with the highest associating SNP in the region (Figure S13), it is possible that another independent SNP in this region is causing the association.

We used multi-trait mixed-model (MTMM) analysis to disentangle genetic and environmental determinants of the phenotypic correlations. We found that the significant correlation between stomata density and stomata size (r = -0.5) had no genetic basis, but had a significant (r=-0.9, $p<0.05$) residual correlation. This suggests that the correlation was not determined by common loci controlling the two traits, but by other, perhaps physical, constraints, or by epistatic alleles at distinct loci. By contrast, the correlation between stomata size and $\delta^{13}C$ (r= -0.18) had a significant genetic basis (Kinship-based correlation, r=-0.58, $p<0.05$).

In order to further investigate the genetic basis for the correlation between stomata size and $\delta^{13}C$, we performed MTMM GWAS, which contrasts three models for each SNP: a null model that includes only global genetic relatedness (kinship), a model including SNP effects common to both traits and a model including both common and trait-specific marker effects (Korte et al., 2012). Contrasting these models reveals SNPs that magnify or decrease the correlation between traits. We did not observe variants increasing genetic correlation between $\delta^{13}C$ and stomata size (Figure S14), suggesting that it is controlled by many loci of small effect. However, in the full model, we observed a marginally significant association on chromosome 4, which de-correlated the two traits. GWAS of $\delta^{13}C$ restricted to the 261

374 individuals used for the MTMM analysis confirmed the QTL on chromosome 4. In this set of
375 genotypes, 2 SNPS, at position 7083610, and position 7083612, exceeded the Bonferroni-
376 corrected significance threshold (α=0.05) (both p=4.8e-09, Figure S15). Allele frequency is
377 14% (37 counts) at these two loci and explains 11% of the observed phenotypic variation. The
378 association is probably due to complex haplotype differences because it coincides with a
379 polymorphic deletion and contains several imputed SNPs. As many as 35 of the 37 accessions
380 carrying the minor allele originated from South Sweden and showed a significantly higher
381 water use efficiency compared to other Southern Swedish accessions (mean difference=1.34;
382 W = 1707, p-value = 1.15e-06; Figure S16). The p-values of associations with $\delta^{13}C$ for the
383 two datasets (310 and 261 accessions) are highly correlated (r=0.87, p<<0.0001, Figure S17).
384 In summary, we detected two genetic variants that significantly associate with $\delta^{13}C$,
385 independent of stomata size, despite the common genetic basis of the two traits.
386
387
388 ## Stomata size and stomata density correlate with geographical patterns of climatic
389 ## variation
390 We used principal component analysis to describe multivariate variation in climatic
391 conditions reported for the locations of origins of the genotypes. We tested the correlation of
392 each measured phenotype with climatic principal components (PC) using a generalized linear
393 model which accounted for genetic population structure (see methods). We found a
394 significant, negative relationship between genetic variation in stomatal size and climatic PC2
395 (Likelihood ratio test Chi-Square (LRT X^2) =9.2784, degrees of freedom (df)=1, p=0.005) and
396 PC5 (LRT X^2= 5.7335, df=1, p=0.02 Figure 3). Climatic PC 2 explained 23.8% of climatic
397 variation and had the strongest loadings (both negative) from temperature and water vapor

pressure (humidity). Climatic PC 5 explained 9% of the climatic variation and mostly increased with increasing spring-summer drought probability ratio and increasing solar radiation. We also found significant climatic predictors for the distribution of genetic variation in stomata density (PC 2: LRT X^2= 8.6612, df=1 p=0.003; PC 5: LRT X^2= 7.3773, df=1, p=0.007; PC 7: LRT X^2= 6.6033, df=1, p=0.01; Figure S18). $\delta^{13}C$ did not correlate with any of the climatic PCs. However, removing population structure covariates from the model revealed significant correlations of $\delta^{13}C$ with climatic PC2 (+, LRT X^2= 7.3564, df=1, p=0.006), PC3 (-, LRT X^2= 3.8889, df=1, p=0.048) and PC4 (+, LRT X^2= 6.6885, df=1, p= 0.009) (Figure S19). PC3 explained 13.7% of climatic variation and principally increased with rainfall and decreased with spring-summer drought probability ratio. PC4 explained 11.4% of the total variation and mostly increased with wind speed. Therefore, the covariation of $\delta^{13}C$ with climatic parameters describing variation in water availability and evaporation in *A. thaliana* is strong but confounded with the demographic history of the species.

Patterns of regional differentiation depart from neutral expectations

Genotypes were divided into five groups (regions) according to their geographic origin (Figure S1). We detected significant phenotypic differentiation among these regions for stomata size (LRT X^2=52.852, df=4, p=9.151e-11, Figure 4). Stomata size was highest in accessions from Central Europe (mean=114 µm²) and significantly lower in accessions from North Sweden (mean=110 µm², General Linear Hypothesis Test (GLHT) z=-2.842, p = 0.0333) and South Sweden (mean=109 µm², GLHT z=-5.781, p<0.001). Spanish accessions also had significantly larger stomata (mean=112 µm²) than South Swedish accessions (GLHT

z=6.044, p<0.001). Variation for stomata density, which is negatively correlated with stomata size, showed a similar but inverted pattern (Figure S20).

Furthermore, we found significant regional differentiation in $\delta^{13}C$ measurements (LR X^2 =58.029, df=4 p=7.525e-12, Figure 4). Highest $\delta^{13}C$ levels (highest WUE) were found in accessions from North Sweden (mean=-34.8) and South Sweden (mean=-35.2), which were significantly higher than in accessions from Spain (mean=-35.7; GLHT South Sweden z= -3.306, p=0.008; GLHT North Sweden z=-3.77, p=0.001) and Western Europe (mean=-36.17; GLHT South Sweden z= -3.108, p=0.015; GLHT North Sweden z=-3.77, p=0.001). Lowest $\delta^{13}C$ levels were found in lines from Central Europe (mean=-36.6), which were significantly lower than in lines from North Sweden (GLHT z=6.223, p<0.001), South Sweden (GLHT z=6.267, p<0.001) and Spain (GLHT z=4.025, p<0.001). These differences are visualized in Figure 4.

The observed regional differences might result either from the demographic history of the regions or from the action of local selective forces. To tease these possibilities apart, the phenotypic differentiation (Q_{ST}) can be compared to nucleotide differentiation at the nucleotide level (Kronholm et al., 2012; Leinonen, McCairns, O'hara, & Merilä, 2013). We examined each pair of regions separately, since they are not equidistant from each other, and calculated F_{ST} distributions for over 70,000 independent SNP markers (spaced at least 1kb apart, see methods) from the 1001-genome project (Alonso-Blanco et al., 2016). For each trait, Q_{ST} exceeded the 95th percentile of the F_{ST} distribution in at least two pairs of regions (Table 1 A-C). We used permutations to calculate a significance threshold for the Q_{ST}/F_{ST}

445 difference (see methods). Significant regional differentiation was pervasive in our sample,
446 with Central Europe and South Sweden being significantly differentiated for all four
447 phenotypes. This analysis suggests that natural selection has contributed to shape the
448 phenotypic differentiation between regions.
449
450
451 Local differences in climate may have imposed regional divergence in stomatal patterning.
452 Thus, we estimated climatic distances between regions using estimates of regional effects
453 extracted from a multivariate analysis of variance. We did not observe significant correlations
454 between phenotypic divergence as measured by Q_{ST} and the climatic distance of the
455 respective regions (Mantel test $p>0.05$ for each of the three traits).
456
457

458 # Discussion

459 ## Genetic variation for stomata patterning segregates in A. thaliana

460 We used high-throughput confocal imaging to characterize stomata patterning in over 31,000
461 images from 870 samples collected from 330 genotypes. Using automated image acquisition
462 and analysis, we could characterize stomata density and stomata size, with an accuracy
463 confirmed by the high correlation with manual estimates. Pavement cells could not be
464 accurately counted, so that stomata indices, which describe the rate of epidermal cell
465 differentiation (Salisbury, 1928), were not quantified. As a result, the genetic diversity of cell
466 differentiation processes was not evaluated. Nevertheless, our approach provides a complete
467 view over the amount of stomata diversity displayed on the leaf surface. This morphological

468 variance is indeed the one that should ultimately have an impact on the stomatal conductance
469 required for photosynthesis and growth. Broad-sense heritability and pseudo-heritability
470 estimates for stomata density, which are 29% and 58%, respectively, are slightly lower than in
471 a previous report of manually counted stomata diversity across a smaller sample chosen to
472 maximize genetic diversity (Delgado et al., 2011). Despite this relatively low heritability,
473 stomata size and stomata density showed a strong negative correlation. This is consistent with
474 earlier reports of studies manipulating regulators of stomata development (Doheny-Adams,
475 Hunt, Franks, Beerling, & Gray, 2012; Franks et al., 2015), but also with studies analyzing
476 stomatal trait variation in in a wide range of species (Franks & Beerling, 2009; Hetherington
477 & Woodward, 2003).
478
479 The extensive genomic resources available in *A. thaliana* (Alonso-Blanco et al., 2016)
480 enabled us to interrogate the genetic basis of trait variation and co-variation, with the help of
481 genome-wide association studies (GWAS) (Atwell et al., 2010). We did not detect any
482 genomic region that associated with stomata density at a p-value beyond the Bonferroni
483 significance threshold and for stomata size there was only one significant association with a
484 very low frequency allele on chromosome 4. Given the heritability of these two traits, this
485 shows that many alleles of low frequency and/or small effect contribute to the variation we
486 observe. Indeed, GWAS studies can detect small effect loci only if they segregate at high
487 frequency (Korte & Farlow, 2013; Wood et al., 2014). Alternatively, multiple independent
488 alleles (allelic series) segregating at causal loci may also play a role.
489
490 Using multi-trait GWAS (Korte et al., 2012), we further investigated the impact of genetic
491 variation on the negative co-variation between stomata size and density. This analysis

492 revealed that genetic similarity does not influence the pattern of co-variation. It implies that
493 either multiple alleles act epistatically on the covariation, or that physical or environmental
494 factors explain the correlation.
495
496
497 ## Polygenic variation in stomata patterning can contribute to optimize physiological
498 ## performance
499 Both stomata development and reactions to drought stress stand under intense scrutiny in *A.*
500 *thaliana* (Bergmann & Sack, 2007; Krasensky & Jonak, 2012; Pillitteri & Torii, 2012;
501 Verslues, Govinal Badiger, Ravi, & M. Nagaraj, 2013). Mutants in stomata density or size
502 have recently been shown to have a clear impact carbon physiology (Franks et al., 2015;
503 Hepworth, Doheny-Adams, Hunt, Cameron, & Gray, 2015; Hughes et al., 2017; S. S.
504 Lawson, Pijut, & Michler, 2014; Masle, Gilmore, & Farquhar, 2005; Yoo et al., 2010; Yu et
505 al., 2008).Yet, the relevance of natural variation in stomatal patterning for facing up with
506 local limitation in water availability had not been documented in this species so far. We
507 provide here concomitant measures of morphological and physiological variation to examine
508 the impact of variation in stomatal patterning on natural variation in carbon uptake. In a small
509 number of populations in the close relative *A. lyrata ssp. lyrata*, smaller stomata size indeed
510 coincided with increased WUE as a plastic response to water limitation (Paccard et al., 2014).
511 By including genome-wide patterns of nucleotide diversity, our analysis presents two major
512 findings: i) the increase in stomata size associates with a decrease in water-use efficiency in
513 *A. thaliana* and ii) this pattern of co-variation has a genetic basis. This shows that, in *A.*
514 *thaliana*, variation in stomata size has the potential to be involved in the optimization of
515 physiological processes controlling the trade-off between growth and water loss.

While variation for stomata size and density displayed a largely polygenic basis, without large effect alleles, we detected two regions in the genome that associated significantly with carbon isotope discrimination. Three previous QTL mapping analyses, including one between locally adapted lines from Sweden and Italy, identified 16 distinct QTLs controlling $\delta^{13}C$ (Juenger et al., 2005; McKay et al., 2008). (Mojica et al., 2016). One of these is caused by a rare allele in the root-expressed gene *MITOGEN ACTIVATED PROTEIN KINASE 12* (*MPK-12)*, (Juenger et al., 2005)(Campitelli, Des Marais, & Juenger, 2016). The two QTL we report here on chromosomes 2 and 4 add two novel loci, raising to 18 the number of genomic regions known to impact $\delta^{13}C$ in *A. thaliana*. The novel loci we report, however, are locally frequent. Individuals carrying the minor alleles of both loci are almost exclusively from South Sweden and display significantly higher $\delta^{13}C$ than other Southern Swedish accessions. Interestingly, the accessions with the minor allele associating with high $\delta^{13}C$ in both QTL did not show decreased stomata size compared to other accessions. Multi-trait GWAS confirmed that these QTL are associated with $\delta^{13}C$ variants that are independent of genetic variation for stomata patterning. We therefore can conclude that, while variation in stomata patterning can contribute to the optimization of carbon discrimination, the reverse does not hold. Carbon isotope discrimination, and hence WUE, can be optimized without modifying stomata patterning. A large array of molecular and physiological reactions is indeed known to contribute to tolerance to drought stress (Krasensky & Jonak, 2012; Verslues et al., 2013). The close vicinity of the chromosome 2 QTL to a non-synonymous mutation in a gene encoding an LEA protein, known to act as a chaperone when cells dehydrate, suggests one possible mechanism by which water-use efficiency might be optimized independently of stomata size and density (Candat et al., 2014; Eriksson, Kutzer, Procek, Gröbner, & Harryson,

2011; Reyes et al., 2005). Variation in rates of proline accumulation in the presence of drought stress or in nutrient acquisition in the root are also among the physiological mechanism that appear to have contributed to improve drought stress tolerance in this species (Campitelli et al., 2016; Kesari et al., 2012).

Adaptive evolution of stomata patterning is suggested by the geographic distribution of genetic variation

Phenotypic variation for stomata patterning and carbon uptake is not uniformly distributed throughout the species range. All three phenotypes we report in this study were significantly differentiated between the five broad regions defined in our sample of 330 genotypes. We performed a comparison of phenotypic and nucleotide levels of divergence in order to evaluate the putative role of past selective events in shaping the distribution of diversity we report (Leinonen et al., 2013; Whitlock & Guillaume, 2009). Because these regions are not equally distant, F_{ST}/Q_{ST} comparisons averaged over all populations may mask local patterns of adaptation (Leinonen et al., 2013). We therefore measured Q_{ST} between pairs of regions and compared them to the distribution of pairwise F_{ST}, using permutations to establish the significance of outlier Q_{ST}. This analysis showed that differentiation between regions was stronger than expected from genome-wide patterns of diversity. Moreover, stomata density and stomata size correlated with climatic principal components, which are most strongly driven by temperature, humidity, solar radiation, and historic drought regimen. The strongest Q_{ST}-F_{ST} differences are found across regional pairs including Central Europe, in particular between Central Europe and South Sweden. This somewhat counterintuitive result is supported by an independent study showing that Swedish genotypes maintain photosynthetic

564 activity for a longer time in the absence of water supply (Exposito-Alonso et al., 2017).
565 Locally adapted genotypes from Southern Sweden have also been shown to display higher
566 water-use efficiency than Italian genotypes (Mojica et al., 2016). This regional difference in
567 *A. thaliana* further coincides with the satellite measurements of historic drought regimen,
568 which show that South Sweden is a region where drought frequency is high in the spring
569 compared to summer. Geographic differences in the seasonal window in which drought is
570 more frequent may select for alternative strategies for facing this threat. In Southern European
571 regions, for example, *A. thaliana* appeared to rely on escape strategies provided by increased
572 seed dormancy (Kronholm et al., 2012). In Northern Europe, increased negative co-variation
573 between flowering time and seed dormancy suggested that the narrow growth season imposes
574 a strong selection on life-history traits (Debieu et al., 2013). Taken together, this suggest that
575 decreased stomata size and, consequently, increased $\delta^{13}C$ may have contributed to adaptation
576 to water limitations in spring in a region where the narrow growth season leaves no room for
577 escape strategies. Indeed, both stomata size and $\delta^{13}C$ associate with historic drought regimen.
578 For $\delta^{13}C$, however, this is only the case when genetic population structure is not included as a
579 covariate. This indicates that local adaptation for water-use efficiency might have also
580 contributed to shape the current population structure. In addition, regional contrasts will mask
581 any pattern of local adaptation occurring at a fine-grained scale within regions. It is therefore
582 possible that we underestimate the magnitude of adaptive differentiation between regions,
583 which could further explain why Q_{ST} / F_{ST} differences did not co-vary with environmental
584 divergence in our dataset.
585
586

Conclusion

This work provides a comprehensive description of the variation in stomata size and density that segregates throughout the range of the annual species *A. thaliana*. Although stomata differentiation is a prominent model for the study of the mechanisms controlling cellular differentiation, not much is known about the importance of stomata size and density for the optimization of gas exchanges. Co-variation with measures of carbon physiology now suggest that stomata size is one of the factors contributing to the local optimization of trade-offs between carbon fixation and limitation of water loss.

This work only examined how stomata patterning impacts physiological performance under conditions where water is not limiting. Future work will have to investigate whether this source of genetic variation also contributes to environmental plasticity, both in stomatal development and in carbon isotope discrimination. The closing of stomata is indeed an important reaction to drought stress, and stomata size is known to influence the rate of stomatal closing (Drake et al., 2013; T. Lawson & Blatt, 2014). In addition, several reports indicate that plants can plastically adjust stomatal development in water-limiting conditions (Fraser, Greenall, Carlyle, Turkington, & Friedman, 2009; Paccard et al., 2014; Xu & Zhou, 2008).

Acknowledgements

We thank Swantje Prahl and Hildegard Schwitte for technical support in microscopy and sample preparation, Maria Graf for technical assistance in $\delta^{13}C$ analysis, Anja Linstädter for advice in the statistical analysis and Angela Hancock for critical comments on the manuscript. This research was supported by the Deutsche Forschungsgemeinschaft (DFG) through grant INST 211/575-1 for the automated confocal microscope, and grant ME2742/6-1 in the realm of SPP1529 "Adaptomics", as well as by the European Research Council with Grant 648617 "AdaptoSCOPE".

References

Ågren, J., & Schemske, D. W. (2012). Reciprocal transplants demonstrate strong adaptive differentiation of the model organism Arabidopsis thaliana in its native range. *New Phytologist*, *194*(4), 1112–1122. https://doi.org/10.1111/j.1469-8137.2012.04112.x

Alonso-Blanco, C., Andrade, J., Becker, C., Bemm, F., Bergelson, J., Borgwardt, K. M., … Zhou, X. (2016). 1,135 Genomes Reveal the Global Pattern of Polymorphism in Arabidopsis thaliana. *Cell*, *166*(2), 481–491. https://doi.org/10.1016/j.cell.2016.05.063

Anderson, V. J., & Briske, D. D. (1990). Stomatal Distribution, Density and Conductance of Three Perennial Grasses Native to the Southern True Prairie of Texas. *The American Midland Naturalist*, *123*(1), 152–159. https://doi.org/10.2307/2425768

Arnold, J. B., Daroczi, G., Werth, B., Weitzner, B., Kunst, J., Auguie, B., … London, J. (2017). ggthemes: Extra Themes, Scales and Geoms for "ggplot2" (Version 3.4.0). Retrieved from https://cran.r-project.org/web/packages/ggthemes/index.html

Atwell, S., Huang, Y. S., Vilhjálmsson, B. J., Willems, G., Horton, M., Li, Y., … Nordborg, M. (2010). Genome-wide association study of 107 phenotypes in Arabidopsis thaliana inbred lines. *Nature*, *465*(7298), 627–631. https://doi.org/10.1038/nature08800

Bakker, J. C. (1991). Effects of humidity on stomatal density and its relation to leaf conductance. *Scientia Horticulturae*, *48*(3), 205–212. https://doi.org/10.1016/0304-4238(91)90128-L

Baxter, I., Brazelton, J. N., Yu, D., Huang, Y. S., Lahner, B., Yakubova, E., … Salt, D. E. (2010). A coastal cline in sodium accumulation in Arabidopsis thaliana is driven by natural variation of the sodium transporter AtHKT1;1. *PLoS Genetics*, *6*(11), e1001193. https://doi.org/10.1371/journal.pgen.1001193

Bergmann, D. C., & Sack, F. D. (2007). Stomatal Development. *Annual Review of Plant Biology*, *58*(1), 163–181. https://doi.org/10.1146/annurev.arplant.58.032806.104023

Browning, B. L., & Browning, S. R. (2009). A Unified Approach to Genotype Imputation and Haplotype-Phase Inference for Large Data Sets of Trios and Unrelated Individuals. *The American Journal of Human Genetics*, *84*(2), 210–223. https://doi.org/10.1016/j.ajhg.2009.01.005

Campitelli, B. E., Des Marais, D. L., & Juenger, T. E. (2016). Ecological interactions and the fitness effect of water-use efficiency: Competition and drought alter the impact of natural MPK12 alleles in Arabidopsis. *Ecology Letters*, *19*(4), 424–434. https://doi.org/10.1111/ele.12575

Candat, A., Paszkiewicz, G., Neveu, M., Gautier, R., Logan, D. C., Avelange-Macherel, M.-H., & Macherel, D. (2014). The Ubiquitous Distribution of Late Embryogenesis Abundant Proteins across Cell Compartments in Arabidopsis Offers Tailored Protection against Abiotic Stress. *The Plant Cell*, *26*(7), 3148–3166. https://doi.org/10.1105/tpc.114.127316

Carlson, J. E., Adams, C. A., & Holsinger, K. E. (2016). Intraspecific variation in stomatal traits, leaf traits and physiology reflects adaptation along aridity gradients in a South African shrub. *Annals of Botany*, *117*(1), 195–207. https://doi.org/10.1093/aob/mcv146

Carroll, S. P., Hendry, A. P., Reznick, D. N., & Fox, C. W. (2007). Evolution on ecological time-scales. *Functional Ecology*, *21*(3), 387–393. https://doi.org/10.1111/j.1365-2435.2007.01289.x

Chater, C., Kamisugi, Y., Movahedi, M., Fleming, A., Cuming, A. C., Gray, J. E., & Beerling, D. J. (2011). Regulatory mechanism controlling stomatal behavior conserved across 400 million years of land plant evolution. *Current Biology: CB*, *21*(12), 1025–1029. https://doi.org/10.1016/j.cub.2011.04.032

Danecek, P., Auton, A., Abecasis, G., Albers, C. A., Banks, E., DePristo, M. A., … Durbin, R. (2011). The variant call format and VCFtools. *Bioinformatics*, *27*(15), 2156–2158. https://doi.org/10.1093/bioinformatics/btr330

Daszkowska-Golec, A., & Szarejko, I. (2013). Open or Close the Gate – Stomata Action Under the Control of Phytohormones in Drought Stress Conditions. *Frontiers in Plant Science*, *4*. https://doi.org/10.3389/fpls.2013.00138

Debieu, M., Tang, C., Stich, B., Sikosek, T., Effgen, S., Josephs, E., … Meaux, J. de. (2013). Co-Variation between Seed Dormancy, Growth Rate and Flowering Time Changes with Latitude in Arabidopsis thaliana. *PLOS ONE*, *8*(5), e61075. https://doi.org/10.1371/journal.pone.0061075

Delgado, D., Alonso-Blanco, C., Fenoll, C., & Mena, M. (2011). Natural variation in stomatal abundance of Arabidopsis thaliana includes cryptic diversity for different developmental processes. *Annals of Botany*, *107*(8), 1247–1258. https://doi.org/10.1093/aob/mcr060

Doheny-Adams, T., Hunt, L., Franks, P. J., Beerling, D. J., & Gray, J. E. (2012). Genetic manipulation of stomatal density influences stomatal size, plant growth and tolerance to restricted water supply across a growth carbon dioxide gradient. *Philosophical Transactions of the Royal Society B: Biological Sciences*, *367*(1588), 547–555. https://doi.org/10.1098/rstb.2011.0272

Drake, P. L., Froend, R. H., & Franks, P. J. (2013). Smaller, faster stomata: scaling of stomatal size, rate of response, and stomatal conductance. *Journal of Experimental Botany*, *64*(2), 495–505. https://doi.org/10.1093/jxb/ers347

Eriksson, S. K., Kutzer, M., Procek, J., Gröbner, G., & Harryson, P. (2011). Tunable membrane binding of the intrinsically disordered dehydrin Lti30, a cold-induced plant stress protein. *The Plant Cell*, *23*(6), 2391–2404. https://doi.org/10.1105/tpc.111.085183

Exposito-Alonso, M., Vasseur, F., Ding, W., Wang, G., Burbano, H. A. A., & Weigel, D. (2017). Genomic basis and evolutionary potential for extreme drought adaptation in Arabidopsis thaliana. *BioRxiv*, 118067. https://doi.org/10.1101/118067

Farquhar, G. D., Hubick, K. T., Condon, A. G., & Richards, R. A. (1989). Carbon Isotope Fractionation and Plant Water-Use Efficiency. In P. W. Rundel, J. R. Ehleringer, & K. A. Nagy (Eds.), *Stable Isotopes in Ecological Research* (pp. 21–40). New York, NY: Springer New York. https://doi.org/10.1007/978-1-4612-3498-2_2

Fick, S. E., & Hijmans, R. J. (2017). WorldClim 2: new 1-km spatial resolution climate surfaces for global land areas. *International Journal of Climatology*.

Fitzgibbon, J., Beck, M., Zhou, J., Faulkner, C., Robatzek, S., & Oparka, K. (2013). A Developmental Framework for Complex Plasmodesmata Formation Revealed by Large-Scale Imaging of the Arabidopsis Leaf Epidermis. *The Plant Cell Online*, *25*(1), 57–70. https://doi.org/10.1105/tpc.112.105890

Fournier-Level, A., Korte, A., Cooper, M. D., Nordborg, M., Schmitt, J., & Wilczek, A. M. (2011). A Map of Local Adaptation in Arabidopsis thaliana. *Science*, *334*(6052), 86–89. https://doi.org/10.1126/science.1209271

Fox, J., Weisberg, S., Friendly, M., Hong, J., Andersen, R., Firth, D., & Taylor, S. (2016). effects: Effect Displays for Linear, Generalized Linear, and Other Models (Version 3.1-2). Retrieved from https://cran.r-project.org/web/packages/effects/index.html

Franks, P. J., & Beerling, D. J. (2009). Maximum leaf conductance driven by CO2 effects on stomatal size and density over geologic time. *Proceedings of the National Academy of Sciences*, *106*(25), 10343–10347. https://doi.org/10.1073/pnas.0904209106

Franks, P. J., Drake, P. L., & Beerling, D. J. (2009). Plasticity in maximum stomatal conductance constrained by negative correlation between stomatal size and density: an analysis using Eucalyptus globulus. *Plant, Cell & Environment*, *32*(12), 1737–1748. https://doi.org/10.1111/j.1365-3040.2009.002031.x

Franks, P. J., W. Doheny-Adams, T., Britton-Harper, Z. J., & Gray, J. E. (2015). Increasing water-use efficiency directly through genetic manipulation of stomatal density. *New Phytologist*, *207*(1), 188–195. https://doi.org/10.1111/nph.13347

Fraser, L. H., Greenall, A., Carlyle, C., Turkington, R., & Friedman, C. R. (2009). Adaptive phenotypic plasticity of Pseudoroegneria spicata: response of stomatal density, leaf area and biomass to changes in water supply and increased temperature. *Annals of Botany*, *103*(5), 769–775. https://doi.org/10.1093/aob/mcn252

Gaut, B. (2012). Arabidopsis thaliana as a model for the genetics of local adaptation. *Nature Genetics*, *44*(2), 115–116. https://doi.org/10.1038/ng.1079

Goudet, J. (2005). hierfstat, a package for r to compute and test hierarchical F-statistics. *Molecular Ecology Notes*, *5*(1), 184–186. https://doi.org/10.1111/j.1471-8286.2004.00828.x

Gowik, U., Bräutigam, A., Weber, K. L., Weber, A. P. M., & Westhoff, P. (2011). Evolution of C4 Photosynthesis in the Genus Flaveria: How Many and Which Genes Does It Take to Make C4? *The Plant Cell*, *23*(6), 2087–2105. https://doi.org/10.1105/tpc.111.086264

Hamilton, J. A., Okada, M., Korves, T., & Schmitt, J. (2015). The role of climate adaptation in colonization success in Arabidopsis thaliana. *Molecular Ecology*, *24*(9), 2253–2263. https://doi.org/10.1111/mec.13099

Hendry, A. P. (2016). *Eco-evolutionary Dynamics*. Princeton University Press.

Hepworth, C., Doheny-Adams, T., Hunt, L., Cameron, D. D., & Gray, J. E. (2015). Manipulating stomatal density enhances drought tolerance without deleterious

effect on nutrient uptake. *The New Phytologist*, *208*(2), 336–341. https://doi.org/10.1111/nph.13598

Hetherington, A. M., & Woodward, F. I. (2003). The role of stomata in sensing and driving environmental change. *Nature*, *424*(6951), 901–908. https://doi.org/10.1038/nature01843

Hothorn, T., Bretz, F., Westfall, P., Heiberger, R. M., Schuetzenmeister, A., & Scheibe, S. (2017). multcomp: Simultaneous Inference in General Parametric Models (Version 1.4-7). Retrieved from https://cran.r-project.org/web/packages/multcomp/index.html

Hughes, J., Hepworth, C., Dutton, C., Dunn, J. A., Hunt, L., Stephens, J., … Gray, J. E. (2017). Reducing Stomatal Density in Barley Improves Drought Tolerance without Impacting on Yield. *Plant Physiology*, *174*(2), 776–787. https://doi.org/10.1104/pp.16.01844

Jombart, T., Kamvar, Z. N., Lustrik, R., Collins, C., Beugin, M.-P., Knaus, B., … Calboli, F. (2016). adegenet: Exploratory Analysis of Genetic and Genomic Data (Version 2.0.1). Retrieved from https://cran.r-project.org/web/packages/adegenet/index.html

Juenger, T. E., Mckay, J. K., Hausmann, N., Keurentjes, J. J. B., Sen, S., Stowe, K. A., … Richards, J. H. (2005). Identification and characterization of QTL underlying whole-plant physiology in Arabidopsis thaliana: δ13C, stomatal conductance and transpiration efficiency. *Plant, Cell & Environment*, *28*(6), 697–708. https://doi.org/10.1111/j.1365-3040.2004.01313.x

Kahle, D., & Wickham, H. (2013). ggmap: Spatial Visualization with ggplot2. *The R Journal*, *5*(1), 144–161.

Kang, H. M., Sul, J. H., Service, S. K., Zaitlen, N. A., Kong, S.-Y., Freimer, N. B., … Eskin, E. (2010). Variance component model to account for sample structure in genome-wide association studies. *Nature Genetics*, *42*(4), 348–354. https://doi.org/10.1038/ng.548

Kesari, R., Lasky, J. R., Villamor, J. G., Marais, D. L. D., Chen, Y.-J. C., Liu, T.-W., … Verslues, P. E. (2012). Intron-mediated alternative splicing of Arabidopsis P5CS1 and its association with natural variation in proline and climate adaptation. *Proceedings of the National Academy of Sciences*, *109*(23), 9197–9202. https://doi.org/10.1073/pnas.1203433109

Kinoshita, T., Ono, N., Hayashi, Y., Morimoto, S., Nakamura, S., Soda, M., … Shimazaki, K. (2011). FLOWERING LOCUS T Regulates Stomatal Opening. *Current Biology*, *21*(14), 1232–1238. https://doi.org/10.1016/j.cub.2011.06.025

Knaus, B. J., Grunwald, N. J., Anderson, E. C., Winter, D. J., & Kamvar, Z. N. (2017). vcfR: Manipulate and Visualize VCF Data (Version 1.4.0). Retrieved from https://cran.r-project.org/web/packages/vcfR/index.html

Kogan, F. N. (1995). Application of vegetation index and brightness temperature for drought detection. *Advances in Space Research*, *15*(11), 91–100. https://doi.org/10.1016/0273-1177(95)00079-T

Korte, A., & Farlow, A. (2013). The advantages and limitations of trait analysis with GWAS: a review. *Plant Methods*, *9*, 29. https://doi.org/10.1186/1746-4811-9-29

Korte, A., Vilhjálmsson, B. J., Segura, V., Platt, A., Long, Q., & Nordborg, M. (2012). A mixed-model approach for genome-wide association studies of correlated traits in structured populations. *Nature Genetics*, *44*(9), 1066–1071. https://doi.org/10.1038/ng.2376

Krasensky, J., & Jonak, C. (2012). Drought, salt, and temperature stress-induced metabolic rearrangements and regulatory networks. *Journal of Experimental Botany*, *63*(4), 1593–1608. https://doi.org/10.1093/jxb/err460

Kronholm, I., Picó, F. X., Alonso-Blanco, C., Goudet, J., & Meaux, J. de. (2012). Genetic Basis of Adaptation in Arabidopsis Thaliana: Local Adaptation at the Seed Dormancy Qtl Dog1. *Evolution*, *66*(7), 2287–2302. https://doi.org/10.1111/j.1558-5646.2012.01590.x

Lambers, H., Chapin, F. S., & Pons, T. L. (1998). Photosynthesis, Respiration, and Long-Distance Transport. In *Plant Physiological Ecology* (pp. 10–153). Springer, New York, NY. https://doi.org/10.1007/978-1-4757-2855-2_2

Lasky, J. R., Marais, D., L, D., Lowry, D. B., Povolotskaya, I., McKay, J. K., … Juenger, T. E. (2014). Natural Variation in Abiotic Stress Responsive Gene Expression and Local Adaptation to Climate in Arabidopsis thaliana. *Molecular Biology and Evolution*, *31*(9), 2283–2296. https://doi.org/10.1093/molbev/msu170

Lawson, S. S., Pijut, P. M., & Michler, C. H. (2014). The cloning and characterization of a poplar stomatal density gene. *Genes & Genomics. 36(4): 427-441.*, *36*(4), 427–441. https://doi.org/10.1007/s13258-014-0177-x

Lawson, T., & Blatt, M. R. (2014). Stomatal Size, Speed, and Responsiveness Impact on Photosynthesis and Water Use Efficiency. *Plant Physiology*, *164*(4), 1556–1570. https://doi.org/10.1104/pp.114.237107

Lawson, T., Kramer, D. M., & Raines, C. A. (2012). Improving yield by exploiting mechanisms underlying natural variation of photosynthesis. *Current Opinion in Biotechnology*, *23*(2), 215–220. https://doi.org/10.1016/j.copbio.2011.12.012

Leinonen, T., McCairns, R. S., O'hara, R. B., & Merilä, J. (2013). QST–FST comparisons: evolutionary and ecological insights from genomic heterogeneity. *Nature Reviews Genetics*, *14*(3), 179–190.

Masle, J., Gilmore, S. R., & Farquhar, G. D. (2005). The ERECTA gene regulates plant transpiration efficiency in Arabidopsis. *Nature*, *436*(7052), 866. https://doi.org/10.1038/nature03835

McDowell, N., Pockman, W. T., Allen, C. D., Breshears, D. D., Cobb, N., Kolb, T., … Yepez, E. A. (2008). Mechanisms of plant survival and mortality during drought: why do some plants survive while others succumb to drought? *New Phytologist*, *178*(4), 719–739. https://doi.org/10.1111/j.1469-8137.2008.02436.x

McKay, J. K., Richards, J. H., Nemali, K. S., Sen, S., Mitchell-Olds, T., Boles, S., … Juenger, T. E. (2008). Genetics of Drought Adaptation in Arabidopsis Thaliana Ii. Qtl Analysis of a New Mapping Population, Kas-1 × Tsu-1. *Evolution*, *62*(12), 3014–3026. https://doi.org/10.1111/j.1558-5646.2008.00474.x

Mojica, J. P., Mullen, J., Lovell, J. T., Monroe, J. G., Paul, J. R., Oakley, C. G., & McKay, J. K. (2016). Genetics of water use physiology in locally adapted Arabidopsis thaliana. *Plant Science*, *251*(Supplement C), 12–22. https://doi.org/10.1016/j.plantsci.2016.03.015

Muchow, R. C., & Sinclair, T. R. (1989). Epidermal conductance, stomatal density and stomatal size among genotypes of Sorghum bicolor (L.) Moench. *Plant, Cell & Environment*, *12*(4), 425–431. https://doi.org/10.1111/j.1365-3040.1989.tb01958.x

Nordborg, M., Borevitz, J. O., Bergelson, J., Berry, C. C., Chory, J., Hagenblad, J., … Weigel, D. (2002). The extent of linkage disequilibrium in Arabidopsis thaliana. *Nature Genetics*, *30*(2), 190–193. https://doi.org/10.1038/ng813

Ohsumi, A., Kanemura, T., Homma, K., Horie, T., & Shiraiwa, T. (2007). Genotypic Variation of Stomatal Conductance in Relation to Stomatal Density and Length in

Rice (Oryza sativa L.). *Plant Production Science*, *10*(3), 322–328. https://doi.org/10.1626/pps.10.322

Paccard, A., Fruleux, A., & Willi, Y. (2014). Latitudinal trait variation and responses to drought in Arabidopsis lyrata. *Oecologia*, *175*(2), 577–587. https://doi.org/10.1007/s00442-014-2932-8

Pearce, D. W., Millard, S., Bray, D. F., & Rood, S. B. (2006). Stomatal characteristics of riparian poplar species in a semi-arid environment. *Tree Physiology*, *26*(2), 211–218. https://doi.org/10.1093/treephys/26.2.211

Pillitteri, L. J., & Torii, K. U. (2012). Mechanisms of Stomatal Development. *Annual Review of Plant Biology*, *63*(1), 591–614. https://doi.org/10.1146/annurev-arplant-042811-105451

Pinheiro, J., Bates, D., DebRoy, S., Sarkar, D., & R Core Team. (2015). *nlme: Linear and Nonlinear Mixed Effects Models*. Retrieved from http://CRAN.R-project.org/package=nlme

Postma, F. M., & Ågren, J. (2016). Early life stages contribute strongly to local adaptation in Arabidopsis thaliana. *Proceedings of the National Academy of Sciences*, *113*(27), 7590–7595. https://doi.org/10.1073/pnas.1606303113

R Development Core Team. (2008). *R: A language and environment for statistical computing*. Retrieved from http://www.R-project.org

Raven, J. A. (2002). Selection pressures on stomatal evolution. *New Phytologist*, *153*(3), 371–386. https://doi.org/10.1046/j.0028-646X.2001.00334.x

Reich, P. B. (1984). Leaf Stomatal Density and Diffusive Conductance in Three Amphistomatous Hybrid Poplar Cultivars. *New Phytologist*, *98*(2), 231–239. https://doi.org/10.1111/j.1469-8137.1984.tb02733.x

Reyes, J. L., Rodrigo, M.-J., Colmenero-Flores, J. M., Gil, J.-V., Garay-Arroyo, A., Campos, F., … Covarrubias, A. A. (2005). Hydrophilins from distant organisms can protect enzymatic activities from water limitation effects in vitro. *Plant, Cell & Environment*, *28*(6), 709–718. https://doi.org/10.1111/j.1365-3040.2005.01317.x

Salisbury, E. J. (1928). I. On the causes and ecological significance of stomatal frequency, with special reference to the woodland flora. *Phil. Trans. R. Soc. Lond. B*, *216*(431–439), 1–65. https://doi.org/10.1098/rstb.1928.0001

Seren, Ü., Grimm, D., Fitz, J., Weigel, D., Nordborg, M., Borgwardt, K., & Korte, A. (2017). AraPheno: a public database for Arabidopsis thaliana phenotypes. *Nucleic Acids Research*, *45*(D1), D1054–D1059. https://doi.org/10.1093/nar/gkw986

Stinchcombe, J. R., Weinig, C., Ungerer, M., Olsen, K. M., Mays, C., Halldorsdottir, S. S., … Schmitt, J. (2004). A latitudinal cline in flowering time in Arabidopsis thaliana modulated by the flowering time gene FRIGIDA. *Proceedings of the National Academy of Sciences of the United States of America*, *101*(13), 4712–4717. https://doi.org/10.1073/pnas.0306401101

Trabucco, A., & Zomer, R. (2010). Global soil water balance geospatial database. *CGIAR Consortium for Spatial Information, Published Online, Available from the CGIAR-CSI GeoPortal at: Http://Www. Cgiar-Csi. Org (Last Access: January 2013)*.

Verslues, P. E., Govinal Badiger, B., Ravi, K., & M. Nagaraj, K. (2013). Drought tolerance mechanisms and their molecular basis. In tthew A. Jenks & P. M. Hasegawa (Eds.), *Plant Abiotic Stress* (pp. 15–46). John Wiley & Sons, Inc. https://doi.org/10.1002/9781118764374.ch2

Vu, V. Q. (2011). A ggplot2 based biplot (Version 0.55).

Weinig, C., Ewers, B. E., & Welch, S. M. (2014). Ecological genomics and process modeling of local adaptation to climate. *Current Opinion in Plant Biology*, *18*(Supplement C), 66–72. https://doi.org/10.1016/j.pbi.2014.02.007

Whitlock, M. C., & Guillaume, F. (2009). Testing for Spatially Divergent Selection: Comparing QST to FST. *Genetics*, *183*(3), 1055–1063. https://doi.org/10.1534/genetics.108.099812

Wickham, H. (2009). *Ggplot2: elegant graphics for data analysis*. New York: Springer.

Wood, A. R., Esko, T., Yang, J., Vedantam, S., Pers, T. H., Gustafsson, S., … Frayling, T. M. (2014). Defining the role of common variation in the genomic and biological architecture of adult human height. *Nature Genetics*, *46*(11), 1173. https://doi.org/10.1038/ng.3097

Wu, C. A., Lowry, D. B., Nutter, L. I., & Willis, J. H. (2010). Natural variation for drought-response traits in the Mimulus guttatus species complex. *Oecologia*, *162*(1), 23–33. https://doi.org/10.1007/s00442-009-1448-0

Xu, Z., & Zhou, G. (2008). Responses of leaf stomatal density to water status and its relationship with photosynthesis in a grass. *Journal of Experimental Botany*, *59*(12), 3317–3325. https://doi.org/10.1093/jxb/ern185

Yoo, C. Y., Pence, H. E., Jin, J. B., Miura, K., Gosney, M. J., Hasegawa, P. M., & Mickelbart, M. V. (2010). The Arabidopsis GTL1 Transcription Factor Regulates Water Use Efficiency and Drought Tolerance by Modulating Stomatal Density via Transrepression of SDD1. *The Plant Cell Online*, *22*(12), 4128–4141. https://doi.org/10.1105/tpc.110.078691

Yu, H., Chen, X., Hong, Y.-Y., Wang, Y., Xu, P., Ke, S.-D., … Xiang, C.-B. (2008). Activated Expression of an Arabidopsis HD-START Protein Confers Drought Tolerance with Improved Root System and Reduced Stomatal Density. *The Plant Cell*, *20*(4), 1134–1151. https://doi.org/10.1105/tpc.108.058263

Data accessibility

Raw image data and image analysis scripts are available upon request and will be stored in a Dryad repository upon acceptance. All phenotypic data is provided in the supplemental material and will be uploaded to the AraPheno database (https://arapheno.1001genomes.org, (Seren et al., 2017) and stored in a Dryad repository upon acceptance. Additionally, we provide an R Markdown file, which contains all figures (except GWAS and MTMM) and the corresponding R code used to create the figures and statistics in the supplemental material. GWAS scripts are available at https://github.com/arthurkorte/GWAS. MTMM scripts are available at https://github.com/Gregor-Mendel-Institute/mtmm.

Genomic data used is publicly available in the 1001 genomes database (Alonso-Blanco et al., 2016)

Author contributions

JdM, AK, and HD conceived the study. HD conducted the experiment and produced phenotypic data for stomata traits. TM and AW were responsible for $\delta^{13}C$ measurements. GM provided data on historic drought regimen. JdM, AK and HD were responsible for the statistical analyses of the data. JdM and HD wrote the manuscript with significant contributions from AK, TM, AW and GM.

Figures & Tables

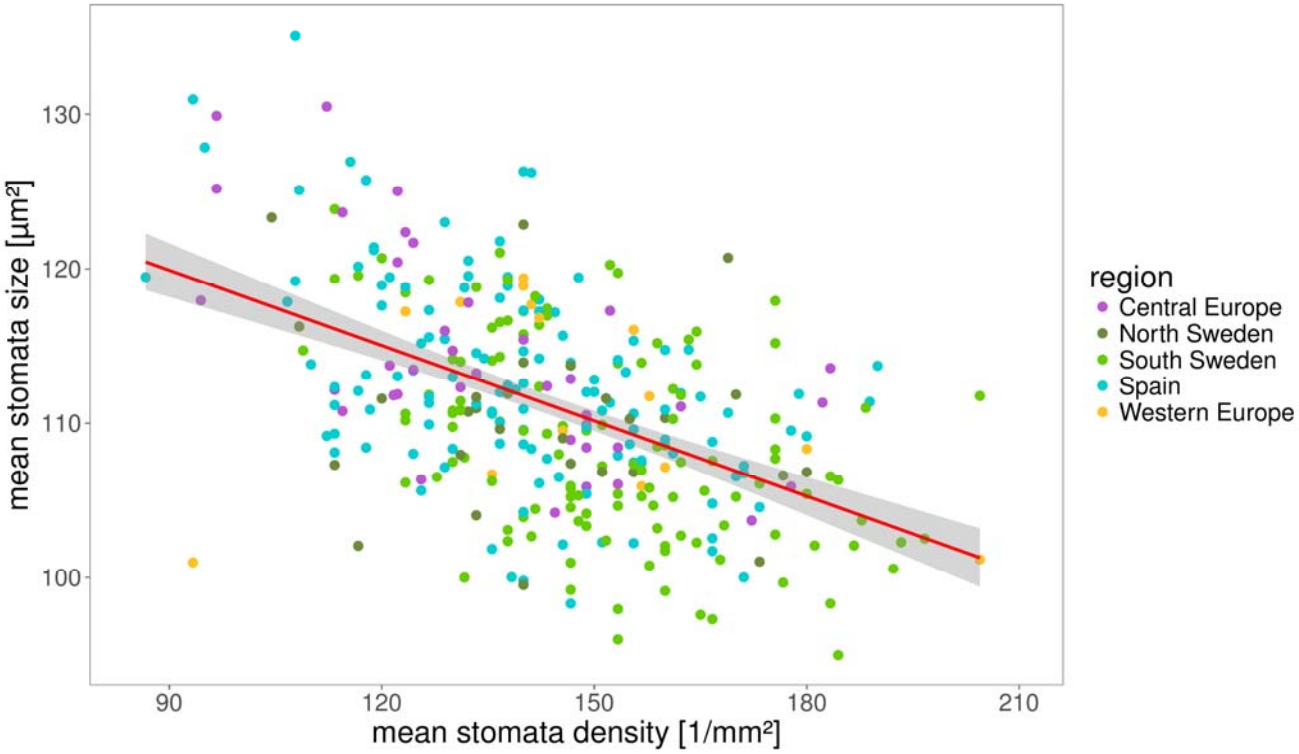

Figure 1: Natural variation in stomata patterning

Stomata density and size were measured for 330 natural genotypes of *A. thaliana*. The plot shows genotypic means of stomata density and stomata size. Dots are colored based on the geographical origin of each accession. The red line shows a linear fit and gray shadows indicate the error of the fit. Pearson's product-moment correlation r=-0.5, p<0.001.

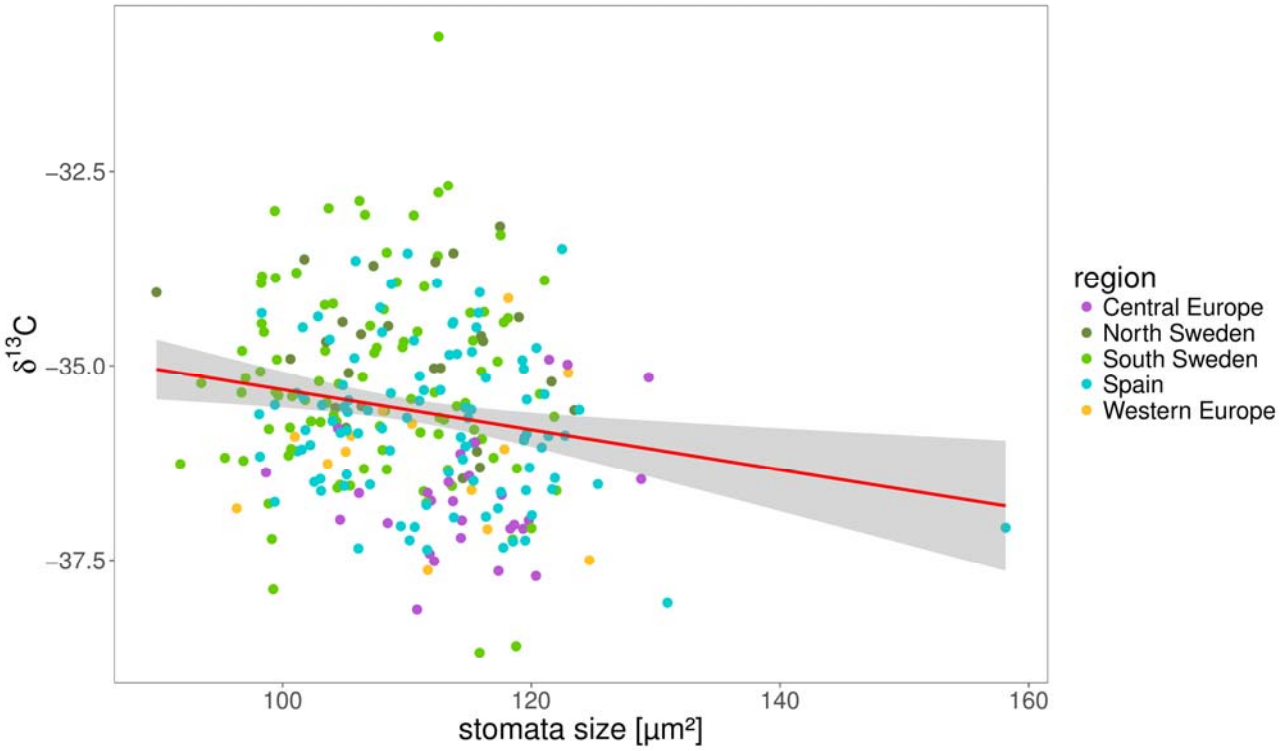

Figure 2: Stomata size correlates with water-use efficiency

$\delta^{13}C$ was measured for all plants in block 1. Plots show correlation of stomata size (block 1 only) with $\delta^{13}C$. $\delta^{13}C$ is expressed as ‰ against the Vienna Pee Dee Belemnite (VPDB) standard. The red line shows a linear fit and gray shadows indicate the error of the fit. Pearson's product-moment correlation: r=-0.18, p=0.004). Correlation of $\delta^{13}C$ and stomata size is not only driven by the Spanish outlier (correlation without outlier: r=-0.16, p=0.009).

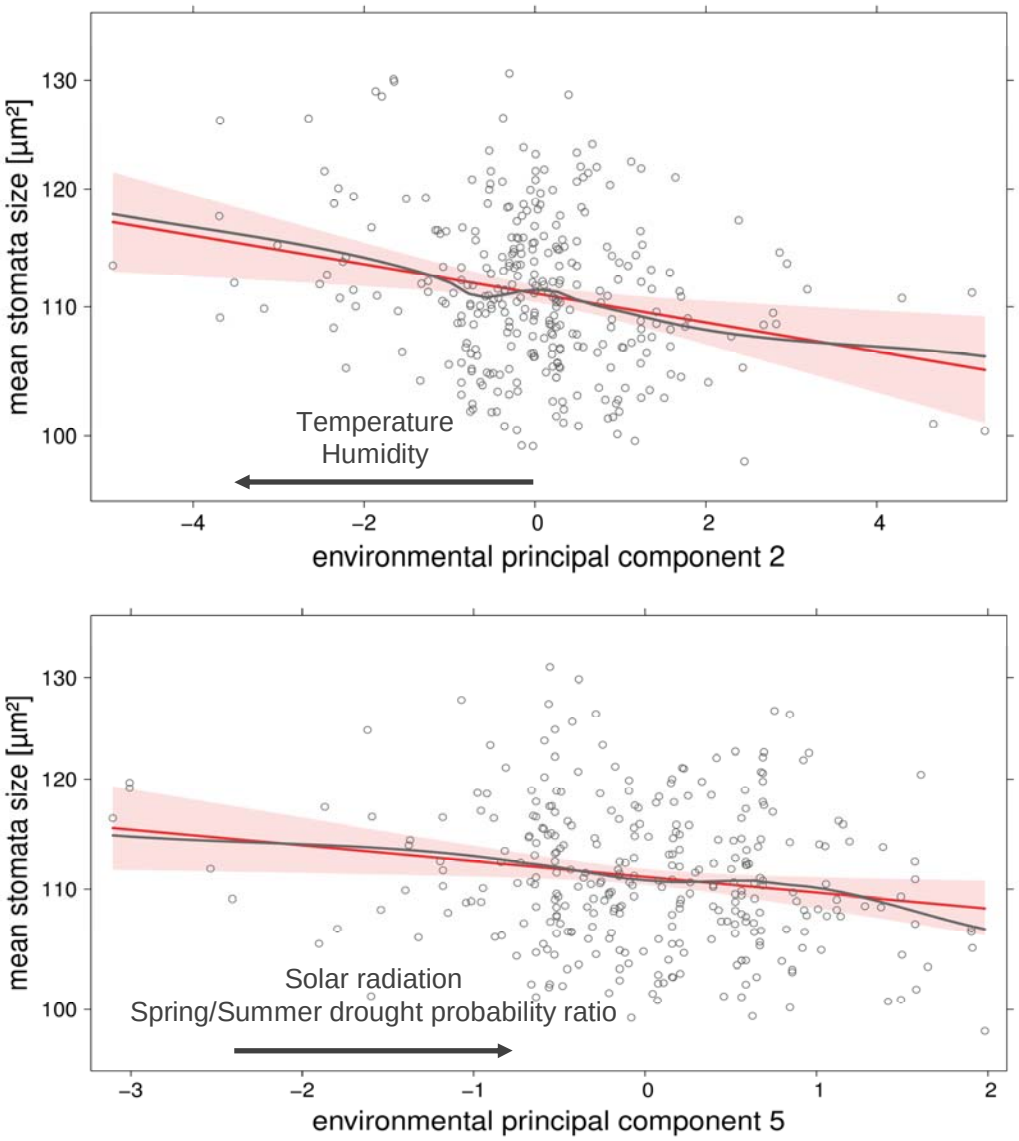

Figure 3: Stomata patterns correlate with geographical patterns of climatic variation

Correlation between stomata patterns and all seven climatic principal components (PCs) was tested for each phenotype using a Generalized Linear Model (GLM) including genetic population structure as described by the 20 first genetic PCs. Plots are effect plots based on the GLM (see methods), showing the correlation between stomata size two climatic PCs. Black arrows indicate correlation with the climatic variables showing the strongest loadings for the respective principal component. Plots show the linear fit (red solid line) and the smoothed fit of partial residuals (gray) of the specific predictor. Gray dots are partial residuals. The red shade shows the error of the linear fit. Both principal components shown here are significant predictors of the respective response variable ($p<0.05$). Results for stomata density are similar but inversed due to negative correlation of the traits (Figure S18).

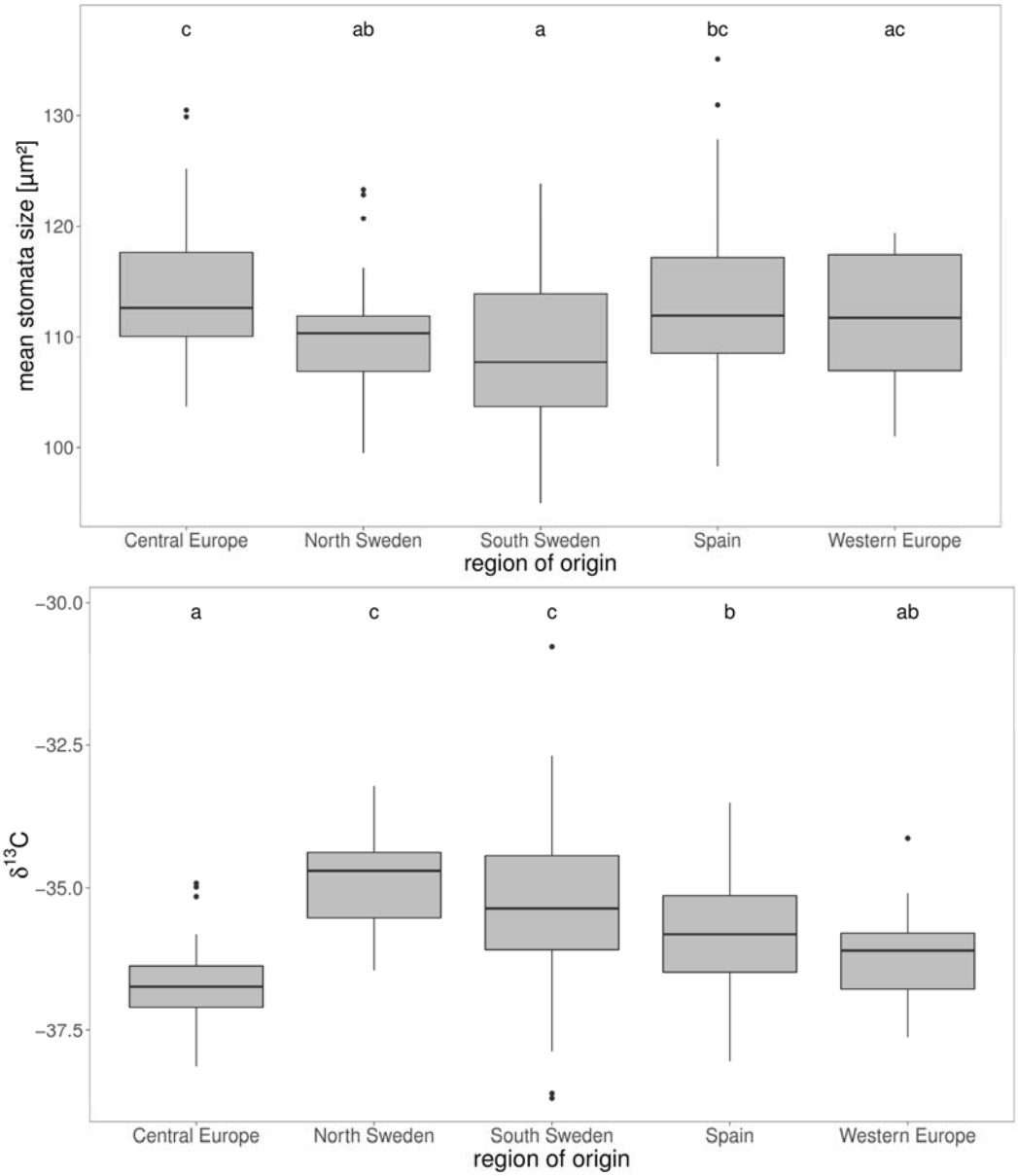

Figure 4: Significant regional differentiation of stomata size and $\delta^{13}C$

A. thaliana accessions were grouped based on their geographical origin. Boxplots show regional differentiation of stomata size (top) and $\delta^{13}C$ (bottom). Significance of differentiation was tested using Generalized Linear Models followed by a post-hoc test. Statistical significance is indicated by letters on top: Groups that do not share a common letter are significantly different. Significance levels: top) a-c, a-bc: $p<0.001$; ab-c: $p<0.05$; bottom) a-c, a-b: $p<0.001$, b-c: $p<0.01$, ab-c: $p<0.05$.

A) Stomata size

Q_{ST} \ Q_{ST}-F_{ST}	Central Europe	North Sweden	South Sweden	Spain	West. Europe
Central Europe		-0.31	**0.24**	-0.17	-0.16
North Sweden	0.17		-0.38	-0.39	-0.53

South Sweden	0.35	0.03		0.06	-0.02
Spain	<0.01	0.07	0.25		-0.18
West. Europe	<0.01	<0.01	0.16	<0.01	

B) Stomata density

Q_{ST} \ Q_{ST}-F_{ST}	Central Europe	North Sweden	South Sweden	Spain	West. Europe
Central Europe		-0.44	**0.20**	-0.18	**0.08**
North Sweden	0.04		-0.29	-0.46	-0.47
South Sweden	0.31	0.11		**0.08**	-0.19
Spain	<0.01	<0.01	0.26		**0.07**
West. Europe	0.24	0.06	<0.01	0.25	

C) **$\delta^{13}C$**

Q_{ST} \ Q_{ST}-F_{ST}	Central Europe	North Sweden	South Sweden	Spain	West. Europe
Central Europe		**0.21**	**0.26**	**0.16**	-0.11
North Sweden	0.7		-0.36	-0.17	-0.04
South Sweden	0.38	0.04		-0.11	-0.01
Spain	0.34	0.28	0.08		-0.08
West. Europe	0.05	0.49	0.17	0.1	

Table 1 A-C: Patterns of regional differentiation depart from neutral expectations

Pairwise Q_{ST} estimates were derived from linear mixed models for all regions. Genome-wide, pairwise F_{ST} distribution was calculated based on 70,000 SNPs for all regions. In the top half of each table, the difference Q_{ST}-F_{ST} for each pair of regions is shown. In the bottom half of each table the Q_{ST} estimate for each pair of regions is shown. Each table represents one phenotype as indicated by table headlines. Significant Q_{ST}-F_{ST} differences are written in bold. The significance threshold is based on the 95th percentile of a distribution of maximum Q_{ST}-F_{ST} values from 1000 random permutations of phenotypic data.